Adsorption of Cobalt (Co^{2+}) from aqueous solution using Nano-scale Graphite Carbon Alginate Bead (NGCAB): Equilibrium, kinetic and thermodynamics studies

Eundo Gee

The Graduate School

Yonsei University

Department of Environmental Engineering

Adsorption of Cobalt (Co^{2+}) from aqueous solution using Nano-scale Graphite Carbon Alginate Bead (NGCAB): Equilibrium, kinetic and thermodynamics studies

A Maters Thesis

Submitted to the Department of Environmental Engineering

and the Graduate School of Yonsei University

in partial fulfillment of the

requirements for the degree of

Master of Science in Environmental Engineering

Eundo Gee

January 2013

The certifies that the Masters

Thesis of Eundo Gee is approved.

Thesis Supervisor : [Byong-Hun Jeon]

[Choi Jaeyoung : Thesis Committee Member #1]

[Dong-Hee Park : Thesis Committee Member #2]

The Graduate School

Yonsei University

January 2013

Table of contents

List of Tables

List of Figures

ABSTRACT

Adsorption of Cobalt (Co^{2+}) from aqueous solution using Nano-scale Graphite Carbon Alginate Bead (NGCAB): Equilibrium, kinetic and thermodynamics studies

Gee, Eundo

Dept. of Environmental Engineering

The Graduate School

Yonsei University

In many industrial activities such as paints, pigment, electronics and mining, the increasing of toxic metal such as Co^{2+} which are discharged into the environment as industrial wastes, represent a serious threat to human health, living resources, and ecological systems. Cobalt expose to through breathing air, drinking water and eating cobalt-containing food that's why cobalt may be easily. In these days, lots of techniques have been appeared for the purification from metal ions such as cobalt in wastewater including adsorption, precipitation, oxidation, ion-exchange and membrane electrolysis, etc. Adsorption, among the above method, is very promising because adsorption is high efficiency, inexpensiveness and simple to handling.

To Co^{2+} removal from aqueous solution, a novel adsorbent was developed by impregnating graphite nano-carbon (GNC) onto alginate bead (AB). Nano-scale Graphite Carbon Alginate Bead (NGCAB) which had physicochemical and spectroscopic properties of the novel adsorbent was characterized and compared with AB. The Co^{2+} adsorption onto NGCAB was quantitatively assessed by determining the kinetics and thermodynamics parameters. The Co^{2+} adsorption capacity was highest at neutral pH condition and the adsorption equilibrium time reached in 10 days using NGCAB.

Increasing the temperature from 288 to 318 K resulted in a 2.5-fold higher Co^{2+} adsorption onto AB, while the thermal dependence of Co^{2+} adsorption on NGCAB was not found. Kinetics studies showed an applicability of pseudo-second-order kinetic model for AB and NGCAB. Monolayer adsorption was the dominant mechanism of Co^{2+} adsorption on AB and NGCAB, which was demonstrated by a better overall fit of Langmuir model to the experimental data. Separation factor (RL) and Freundlich constant (n) were well in the range of values for favorable adsorption. Thermodynamics studies revealed that Co^{2+} adsorption onto AB and NGCAB was endothermic and spontaneous processes. Positive values of entropy indicate randomness in the solid/aqueous phases and the activation energy (Ea) fits in the range of chemisorption.

Key words : Adsorption, Cobalt, Alginate bead, Nano

1. Introduction

In many industrial activities such as paints, pigment, electronics and mining [1], the increasing of toxic metal such as Co^{2+} which are discharged into the environment as industrial wastes, represent a serious threat to human health, living resources, and ecological systems [2]. Cobalt expose to through breathing air, drinking water and eating cobalt-containing food that's why cobalt may be easily [3]. In these days, lots of techniques have been appeared for the purification from metal ions such as cobalt in wastewater including adsorption, precipitation, oxidation, ion-exchange and membrane electrolysis, etc. Adsorption, among the above method, is very promising because adsorption is high efficiency, inexpensiveness and simple to handling. There are many materials to remove heavy metal such as boron impurity [4], palygorskite[5], resin[6], silica gel[7], microcapsules[8], cellulose/chitin bead[9] and chitosan-coated perlite bead[10]. Especially many studies are used as adsorptive such as bead containing alginate or alginic acid. Alginic acid or alginate is given to family of linear polysaccharides containing 1, 4- linked ß-D-mannuronic (M) and R-L-guluronic (G) acid residues arranged randomly along the chain [11]. Polyguluronic acid residues for divalent metals, Ca^{2+} especially earily, are explained as "zigzag"structure.

The alginates choose an adopted solution network via between chain dimerization of the polyguluronic sequences in the existence of Ca^{2+} or their divalent cations of similar size [12].

Recently, nanomaterials have been reported to removal diverse pollutants by adsorption [13]. Nano scale and nanoparticle are more effective and promising adsorbent, that's because those materials have large surface volume/area and reactivity [14-15]. Especially carbon nano structures such as carbon nano tubes (CNTs) and fullerene have earned attraction from many researchers because they have inherent applicability [16]. CNTs and fullenrene have a strong Van der Waals attraction force of aggregation so they have limited to applications.

In order to enhance not only adsorption capacity but also economic feasibility and mechanical strength, alginate bead have been changed such as sodium dodecylbenzebe fulfonate entrapment alginate bead [17], blended chitosan – alginate bead [18], entrapped activated carbon with alginate beads [19] and magnetic alginate bead [20].

In present research, we had developed a novel adsorbent by incorporating GNC into AB matrix, designated as alginate beads impregnated with Nano-scale Graphite Carbon Alginate Bead (NGCAB). The physicochemical and spectroscopic characteristics of NGCAB were examined and compared with those of AB. The developed adsorbent was testified for Co^{2+} removal. Equilibrium, thermodynamics and kinetics parameters for Co^{2+} adsorption on NGCAB were comparatively evaluated with those of AB.

2. Theoretical Background

2.1. Cobalt sources and pollution

Cobalt is relatively unique element found in the earth's surface with of approximately 25 μg/g of concentration. Although it occurs naturally in the environment, because anthropogenic activity immoderate amounts of cobalt are released from coal combustion and mining, processing of cobalt-containing ores and the production and use of cobalt chemicals. Cobalt has variety of uses: as a metal in electroplating, because of its hardness and resistance to oxidation, in alloys with iron, nickel and other metals, and also in magnet and stainless steels. Its salts have been used for centuries for the production of blue colors in porcelain, glass, pottery, and enamels, while compounds are used as paint pigments [21]. Radioactive, artificial isotope cobalt-60 is an important gamma-ray source and is used extensively as a tracer and radiotherapeutic agent. In small amounts cobalt is essential for human health, because it is a part of vitamin B^{12} [22]. However, higher concentrations of cobalt may damage human health. Soils near mining and melting facilities may contain very high amounts of cobalt. Once it has entered the environment, it may react with other particles or adsorb on soil and sediments. Under acidic conditions, cobalt becomes mobile causing its accumulation in plants and in animals and humans that eat these plants. Health effects may also be produced by radiation of radioactive cobalt isotopes. ^{60}Co is formed in a nuclear reactor by the (n, γ) reaction of the Co present as an impurity in the metals used, and can also be present in the waste water effluents [23].

2.2. Cobalt removal technology

Various toxic heavy metal ions, especially cobalt, discharged through different industrial activities, constitute one of the major causes of water pollution. Heavy

metal residues in contaminated habitats may accumulate in microorganisms, aquatic flora and fauna, which in turn, may enter into the human food chain and result in health problems [24]. Treatment processes for metal contaminated waste streams include chemical precipitation, ion exchange, membrane filtration, coagulation-flocculation, and adsorption [25].

2.2.1 Chemical precipitation

Chemical precipitation is effective and the most widely used process in industry because it is relatively simple and inexpensive to operate. In precipitation processes, chemicals react with heavy metal ions to form insoluble precipitates. The forming precipitates can be separated from the water by sedimentation or filtration. And the treated water is then decanted and appropriately discharged or reused. The conventional chemical precipitation processes include hydroxide precipitation and sulfide precipitation.

The most widely used chemical precipitation technique is hydroxide precipitation due to its relative simplicity, low cost and ease of pH control [26]. The solubilities of the various metal hydroxides are minimized in the pH range of 8.0 - 11.0. The metal hydroxides can be removed by flocculation and sedimentation. A variety of hydroxides has been used to precipitate metals from wastewater, based on the low cost and ease of handling, lime is the preferred choice of base used in hydroxide precipitation at industrial settings [27].

Sulfide precipitation is also an effective process for the treatment of toxic heavy metals ions. One of the primary advantages of using sulfides is that the solubilities of the metal sulfide precipitates are dramatically lower than hydroxide precipitates and sulfide precipitates are not amphoteric. And hence, the sulfide precipitation process can achieve a high degree of metal removal over a broad pH range compared with hydroxide precipitation. Metal sulfide sludges also exhibit better

thickening and dewatering characteristics than the corresponding metal hydroxide sludges [28].

2.2.2 Ion exchange

Ion-exchange processes have been widely used to remove heavy metals from wastewater due to their many advantages, such as high treatment capacity, high removal efficiency and fast kinetics [29]. Ion-exchange resin, either synthetic or natural solid resin, has the specific ability to exchange its cations with the metals in the wastewater. Among the materials used in ion-exchange processes, synthetic resins are commonly preferred as they are effective to nearly remove the heavy metals from the solution [30].

The most common cation exchangers are strongly acidic resins with sulfonic acid groups ($-SO_3H$) and weakly acid resins with carboxylic acid groups (-COOH). Hydrogen ions in the sulfonic group or carboxylic group of the resin can serve as exchangeable ions with metal cations. As the solution containing heavy metal passes through the cations column, metal ions are exchanged for the hydrogen ions on the resin with the ion-exchange process.

2.2.3 Membrane filtration

Membrane filtration technologies appeared high efficiency for heavy metal removal as easy operation and space saving with different types of membranes. The membrane has several types which are ultrafiltration, reverse osmosis, nanofiltration and electrodialysis to remove metals from the wastewater [31].

Ultrafiltration has large pore sizes of membranes than dissolved metal ions in the form of hydrated ions or as low molecular weight complexes, so these ions could

pass through membrane [32]. To overcome some problem of pore size, the micellar enhanced ultrafiltration (MEUF) [33] and polymer enhanced ultrafiltration (PEUF) [34] was proposed. MEUF was first introduced by Scamehorn et al. in the 1980s for the removal of dissolved organic compounds such as 4-tert-butyl-phenol and multivalent metal ions such as calcium and zinc from aqueous streams. Organic compounds are solubilized in the micelle interior and the metal ions get trapped on the surface of the oppositely charged micelles by electrostatic interaction [35].

Proposed PEUF is a practicable method to separate a variety of metal ions from aqueous phase, also PEUF uses water-soluble polymer for complexing metal ions and form a macromolecular, having a higher molecular weight than the molecular weight cut off of the membrane. The macromolecular will be retained when they are pumped through UF membrane. After that, retentate can be treated in order to recover metallic ions and to reuse polymeric agent. The main concern of the previous PEUF studies was to find suitable polymers to achieve complexation with metal ions [36]. The reverse osmosis (RO) process which uses a semi-permeable membrane is one of the techniques able to remove a wide range of dissolved species from water and is being purified to pass through membrane but major problem of RO is the high energy expenditure because of the pumping pressures [37]. Between UF and RO, nanofiltration (NF) is the intermediate process and is a removal well for rejection of heavy metal for example nickel, chromium, copper and cobalt [38]. NF process has many advantages such as operation, reliability, low energy expenditure and high efficiency.

2.2.4 Coagulation-flocculation

By water treatment method, coagulation is one of the most important. The main objects of coagulation are the hydrophobic colloid and suspended particle which

consist of insoluble substances. The soluble heavy metals ions are pollutant in water which is impracticable to remove by coagulant. They can be adsorbed onto particles, or become particles by hydrolysis. Therefore, the heavy metal content of water can be reduced to some extent by coagulation [39-40].

The polyaluminium chloride (PAC), polyferric sulfate (PFS) and polyacrylamide (RAM) is widely used in the wastewater by treatment flocculants, but in these days, many new flocculants are invested using chitosan with mercaptoacetic acid [41]. Flocculation method is the reaction of polymers to form bridges between the flock and bind the particles into large agglomerates of clumps. Once suspended particles are flocculated into larger particles, they can usually be removed or separated by filtration, straining or floatation.

2.3 Adsorption

Adsorption can be defined as the accumulation of a substance or material at an interface between the solid surface and the bathing solution. Adsorption can include the removal of solute (a substance dissolved in a solvent) molecules from the solution, solvent (continuous phase of a solution, in which the solute is dissolved) from the solid surface, and attachment of the solute molecule to the surface. Adsorption does not include surface precipitation or polymerization (formation of small multinuclear inorganic species such as dimers or trimmers) processes. Adsorption, surface precipitation, and polymerization are all examples of sorption, a general term that is used when the retention mechanism at a surface is unknown.

It would be useful before proceeding any further to define a number f terms pertaining to retention (adsorption/sorption) of ions and molecule. The adsorbate is the material that accumulates at an interface, the solid surface on which the adsorbate accumulates is referred to as the adsorbent, and the molecule or ion in

solution that has the potential of being adsorbed is the adsorptive. If the general term sorption is used, the material that accumulates at the surface the solid surface, and the molecule or ion in solution that can be sorbed are referred to as sorbate, sorbent and sorptive, respectively.

Adsorption is one of the most important chemical processes. It determines the quantity of plant nutrients, metals, pesticides and other organic chemicals that are retained on surfaces and therefore is one of the primary processes that affect transport of nutrients and contaminants. Both physical and chemical forces are involved in adsorption of solutes from solution. Physical forces include van der Waals force (e.g., partitioning) and electrostatic outer-sphere complexes (e.g., ion exchange). Chemical forces result from short-range interactions that include inner-sphere complexation that involves a ligand exchange mechanism, covalent bonding and hydrogen bonding [42].

The sorption rate is known to be controlled by several factors including the following;(I) diffusion of the solute from the solution to the film surrounding the particle, (II) diffusion from the film to the particle surface (external diffusion), (III) diffusion from the surface to the internal sites (surface diffusion or pore diffusion) and (IV) uptake which can involve several mechanisms such as physic-chemical sorption, ion exchange, precipitation or complexation [43].

2.4 Alginate bead and Nano-size carbon

Many researchers were invented for removal efficiently heavy metal ion in the way that bead and gel. By so doing, beneficent material could capture/entrap in a bead and has many advantages which are easy to use, mobility in water and existence of surface area. By Xiaoli Li [44], adsorbent of bead was studied to obtain material consequently macroporous bead adsorbents based on poly (vinyl alcohol)/chitosan. This indicated the hydrophilic character of the studied beads,

which facilitated the adsorption of heavy metals. Judging from the BET results, PVA/CS beads exhibited higher surface area than the beads without CS, which would provide large interface between the adsorbents and heavy metal ions in aqueous solution. The various adsorbent of bead was developed for example magnetic polymer bead [45], gellan gum gel beads [46], chitosan hydrogel beads [47], Poly (ethylene glycol dimethacrylate-n-vinyl imidazole) beads [48], and biomass filled porous epoxy beads [49] and chitosan beads [50]. Among this beads, alginate bead would use by adsorbent to adsorb heavy metal ion commonly.

Mostly alginate bead was consisted of alginic acid which occurs in all brown algae. Alginic acid or alginate, the salt of alginic acid, is the common name given to a family of linear polysaccharides containing 1,4-linked b-d-mannuronic (M) and a-lguluronic (G) acid residues arranged in a non-regular, blockwise order along the chain [51]. The salts of alginic acid with monovalent ions (alkali metals and ammonium) are soluble, whereas those with divalent or polyvalent metal ions (except Mg^{2+}) and the acid itself are insoluble [52].

In alginate different, M and G which are the polymer conformation of the two block residues also two constituents changes according to the genus of the algae from extracted polysaccharide. Furthermore, variations in M:G ratio exist from species to species [53]. The affinity of alginates for divalent cations such as Pb^{2+}, Cu^{2+}, Cd^{2+}, Zn^{2+} and Ca^{2+} increased with the guluronic acid content. The selectivity coefficients for the ion-exchange reaction between sodium and divalent metals were determined for two alginates and confirmed the higher affinity of guluronic acid rich alginates for divalent metals. The higher specificity of polyguluronic acid residues for divalent metals is explained by its ‘‘zigzag’’ structure which can accommodate the Ca^{2+} (and other divalent cations) ion more easily. Alginates can consist in interchain dimerization of the polyguluronic sequences through divalent cation such as present of calcium. The rodlike form of the poly-l-guluronic sections results in an alignment of two chain sections yielding an array of coordination sites, with cavities suitable for calcium and other

divalent cations because they are lined with the carboxylate and other oxygen atoms of G residues. This description is known as the ''egg-box'' model [54]. As a result, several different chains may become interconnected and this promotes gel network formation. The higher the degree of linkage that the grater the resulting viscosity.

The nano-size material is a new functional material, which has attracted much attention due to its special properties. Most of the atoms on the surface of the nanoparticles are unsaturated and can easily bind with other atoms. Nanoparticles have high adsorption capacity. Besides, the operation is simple, and the adsorption process rapid. So there is a growing interest in the application of nanoparticles as adsorbents [55]. With the emergence of nano science and technology in the last decade, research has been initiated to exploit the unusual and unique properties of carbon nanotubes (CNMs). CNMs may exist in several forms, such as, single-walled carbon nanotubes (SWCNTs), multi-walled carbon nanotubes (MWCNTs), carbon beads, and carbon fibres and nanoporous carbon. CNMs have been studied widely for potential applications in catalyst supports, optical devices, quantum computer, and biochips. However, their sorption potential has not been studied extensively. CNMs are engineered materials targeted to exhibit unique surface morphologies; hence, they may prove to be good sorbents [56]. Moreover, by combination of alginate bead high adsorption capacity could demonstrate in table 0. To enhance maximum amount of adsorptive, many researcher used various material as adsorbent with alginate.

Table 1. Comparison with other adsorbents about adsorbed amount.

Adsorbents	Adsorbed ion	Q_{max} (mg/g)	Reference
magnetic alginate microcapsules	Ni(II)	30.51	[8]
magnetic alginate bead	Co(II)	30.72	[57]
activated carbon -containing alginate	Cd(II)	88	[58]
alginate-chitosan hybrid gel bead	Co(II)	3.45	[59]
metal oxide entrapped alginate bead	As(V)	41.6	[60]

3. Materials and methods

Alginic acid, sodium salt was purchased from Aldrich and used without further purification. Dissolution of $CaCl_2 \cdot 2H_2O$ and $Co(NO_3)_2 \cdot 6H_2O$ in deionized water prepared calcium(II) and cobalt(II) solutions, respectively and purchased Sigma. Nano-size carbon colloid was extracted from isotropic graphite.

3.1 Adsorbent preparation

3.1.1 Preparation of nano-size carbon solution

For manufacturing nano-size carbon colloid, 95 percent purity graphite was used. Three graphite plates were located between one cathode and two anodes. There are two cathodes at both ends, thereby increasing efficiency as increasing the surface of working electrodes. Nano-size carbon colloid producers were consisted of plastic containing distilled water as an electrolyte and electrolytic cell 120 x 140 x 105mm (W, H, Th). It's more economical to manufacture carbon nano colloid using distilled water. An electrolytic cell was installed on the agitator and electrolyte includes the creating nano carbon particle by electrolysis from electrode. The electric power applied to the electrodes are DC 15 ~ 30 V. Big particles and fine particles are blended because it's necessary to filtering by paper filter(model 540, 125 mm Ø, Whatman Inc.).

3.1.2 Preparation of alginic acid solution

The alginic acid stock solution is prepared by dissolving alginic acid, sodium salt in volume of distilled water (5 wt. %). It's important to making bead to choose viscosity variations between 20,000 ~ 40,000 cps that's why viscosity variations decided bead's hardenability. The weight average molar weight (Mw) and the

number average molar weight (Mn) of alginate are respectively equal to $1.65x10^5$ and $9.65x10^4$ $gmol^{-1}$, leading to polydispersity indice (Ip) equal to 1.7.

3.1.3 Preparation of NGCAB

Alginic acid solution is hardened immediately while alginate structure have "zigzag" structure by divalent metal ions which can influence upon cross-linking such as Pb^{2+}, Cu^{2+}, Cd^{2+}, Zn^{2+}, Ca^{2+}, etc. Before the cross-linking to making bead [11-12], prepared alginic acid solution and nano-size carbon solution are mixed during 12 hours. 0.05M calcium chloride solution was stirring on the agitator, and then mixed alginic acid and nano-size carbon solution are dropped at a proper distance between separatory funnel and $CaCl_2$ solution. For the making of a fixed size, separatory feunnel is used with 5ml pipet tip into contacting end of the separatory funnel. Beads produced by its devices are neglected in the $CaCl_2$ solution over 24 hours because it should allow at least 24 hours for harden and cross-link fully. After being washed using distilled water several times, it should storage to use adsorption experiments.

3.2 Adsorption experiments

The adsorption experiments were carried out in 50ml conical tubes using 10g/L cobalt solution under agitation on shaker at 100 rpm. Adsorbents were used in NGCAB and Alginate Bead (AB) to compare with their efficiency Stock solution (1,000mg/L) of Co^{2+} ion was prepared into distilled water. In order to determine the effect of each parameters for examples time, pH, temperature and initial Co^{2+} ion concentration of solution. Except for pH effect experiment initial pH of the Co^{2+} solution was adjusted to 7.0±0.5 by adding negligible volumes of 0.1 or 0.01M HNO_3 of NaOH. After shaking the NGCAB was removed by filtration

through 0.45µm syringe PVDF filter (PALL, USA) and solution pH was checked. The pH was measured using a benchtop pH/EC/ORP meter (Mettler Toledo, USA). To measuring initial and final Co^{2+} concentration, ICP-OES (Inductively coupled plasma-optical emission spectrophotometer, 730-ES, Varian, USA) was used after previously to the acidification. The adsorption capacities (mg/g) of NSCAB were calculated as follows:

$$q_e = \frac{(C_o - C_e) \times V}{m} \quad (1)$$

Where C_i and C_e are the initial and the equilibrium concentrations respectively (mg/L), while M (g) and V (L) represent the weight of the adsorbent and the volume of the solution respectively. The pH studies were conducted at different pH between 2 and 9 under ambient temperature (298 K) condition. The initial pH of adsorbate solution (C_o = 0.10 mg/L) was adjusted using diluted HCl and NaOH solutions. The contact time studies were carried out by varying adsorbate concentration (0.10 – 200 mg/L) and temperature (288 – 313 K), while isotherm studies were performed at different adsorbate concentrations ranging from 0.01 to 200 mg/L.

4. Result and discussion

4.1 Nano-size carbon colloid and NGCAB characterizations

In this study transmission electron microscope (TEM, Leo 912A 8B OMEGA EF-TEM, Carl Zeiss Germany) was conducted to know the nano-size carbon particle. Nano-size carbon colloid, which is round form, was detected and carbon colloid was made up of less than 20 nm in size (fig. 1(a)). TEM images of AB and NGCAB in Fig. 1(a) and (b) shows what compare having smooth surface only alginate bead and having rough surface alginate bead nano-size carbon colloid combined. At irregular distance, many black spots are appeared; thus average size, 80 – 100nm, of nano-size carbons were found by form of size fraction.

Particle size distribution of nano-size carbon colloid (Nano Sight, UK) was measured for average particle ranges. Nano-size of particle was distributed variously that range of distribution is 10 nm to 220 nm, yet major average diameter of particles showed around 50nm.

Measurements of NGCAB pH_{pzc} were determined by potentiometric titration, the results are shown in fig. 2. pH_{pzc} value of NGCAB is 6.8±0.03. This result can draw comparisons with other carbon material and is similar pH_{pzc} value in close to the neutral pH whereas less than 1.0 pH_{pzc} value of AB was measured. The kind of two measured beads displayed, depending on the pH, negative and positive charge. To adsorb Co^{2+} on the surface negative charge are favorable because of electrostatic interactions.

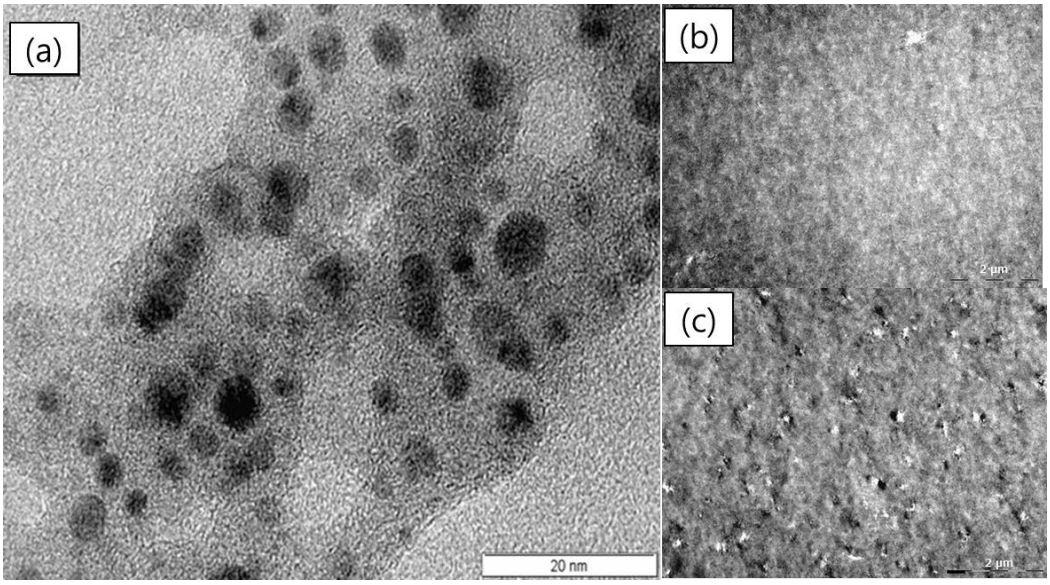

Figure 1. TEM image of nano-size carbon colloid(a), AB surface (b) and NGCAB surface (c)

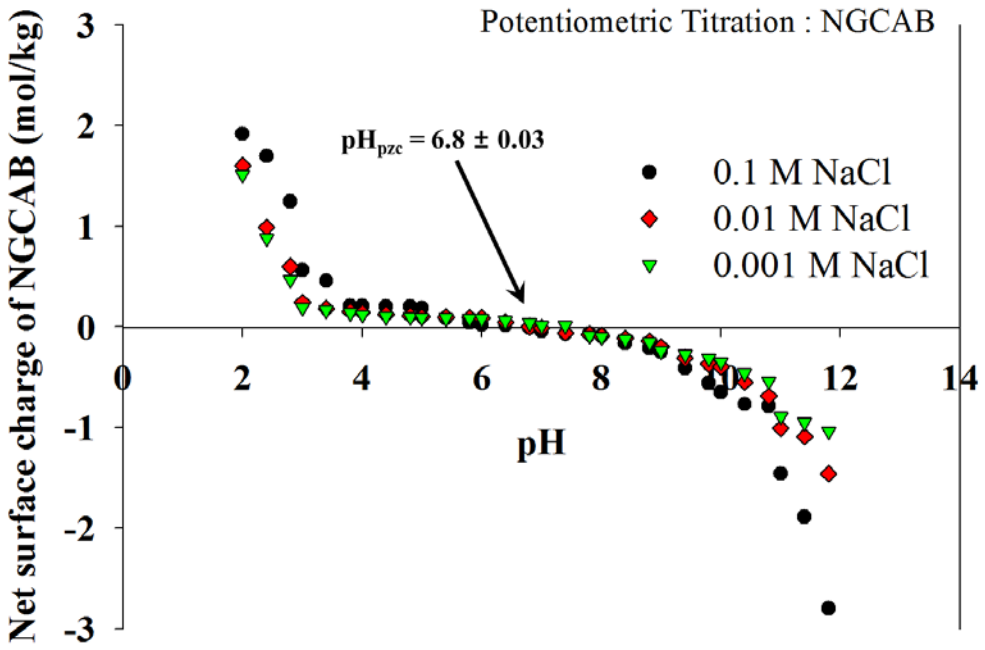

Figure 2. Net surface charge of NGCAB at three ionic strengths as determined by the PZC titration procedures

EDX analysis was measured by Field Emission scanning Electron Microscope (FESEM, Hitachi, SU-70, KBSI Gangneung Center) equipped with an energy dispersive X-ray spectroscopy (EDX). Consequently NGCAB has carbon atomic 82.02% and calcium 4.55 % (a) since it used cross-linking between alginate structures. After cobalt adsorption cobalt 4.12% was detected (b) so it is useful to confirm that Co^{2+} was adsorbed well.

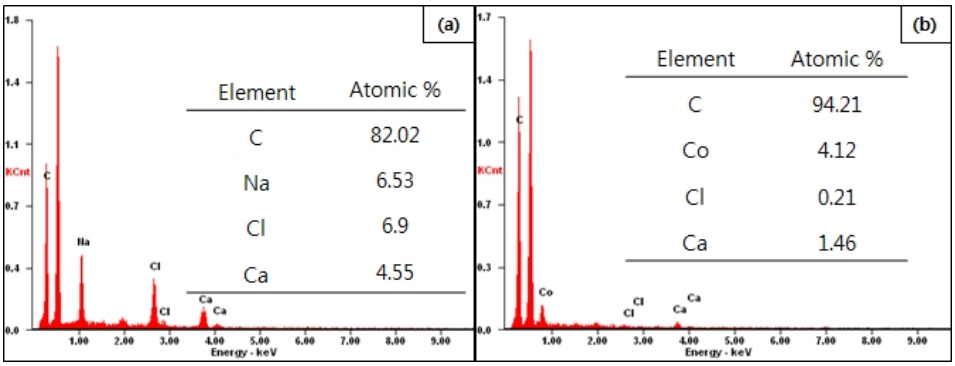

Figure 3. SEM-EDX analysis of nano-size carbon alginate bead (a) and after Co^{2+} adsorption

4.2.1 FT-IR spectra

Samples were dried first and then ground before performing FT-IR analysis. FT-IR spectra were recorded on a Perkin-Elmer Spectrometer. The FT-IR spectra (fig. 5) were collected from 2000 to 800cm^{-1} range in the transmission mode with 4cm^{-1} resolution over 40 scans. The alginate polymer bead does not exhibits the adsorption ability of Co ion and IR spectra also shows no changes with coexisted with Co ion. The IR spectra of alginate polymer bead with and without nano carbon shows very similar pattern. It is also observed that, the peaks of stretching of C=O of carboxylic group of alginic acid when the proton was displaced by a mono-valent ion (sodium) appeared at 1601 and 1432 cm-1, respectively. These peaks were assigned for asymmetric and symmetric stretching vibration of free carboxyl group of sodium alginate [61-62].

After addition of Co ion, the new peaks are appeared at 1730 cm^{-1} and grow as concentration of Co ion increased. If the mono-valent sodium ion at alginate displaced by a divalent ion (Co^{2+}), the peaks of stretching of C=O of carboxylic group will be shifted to 1620 and 1426 cm^{-1}, respectively. And, it is known that the stretching of C=O of protonated carboxylic group of alginic acid occurs at 1730 and 1609cm^{-1}, respectively in fig. 4. Thus upon addition of Co ion, it is not occur a displacement of sodium ion of alginate with Co ion. The peak at 1609 cm^{-1} for protonated carboxylic acid of alginic acid was shifted to 1730 cm^{-1} due to the removal of sodium from alginate polymer. As in the present case, divalent metal ions (Co) had removed sodium ions in the sodium alginate, the charge density, the radius and the atomic weight of the cation site were subsequently changed, creating a new environment around the carbonyl group.

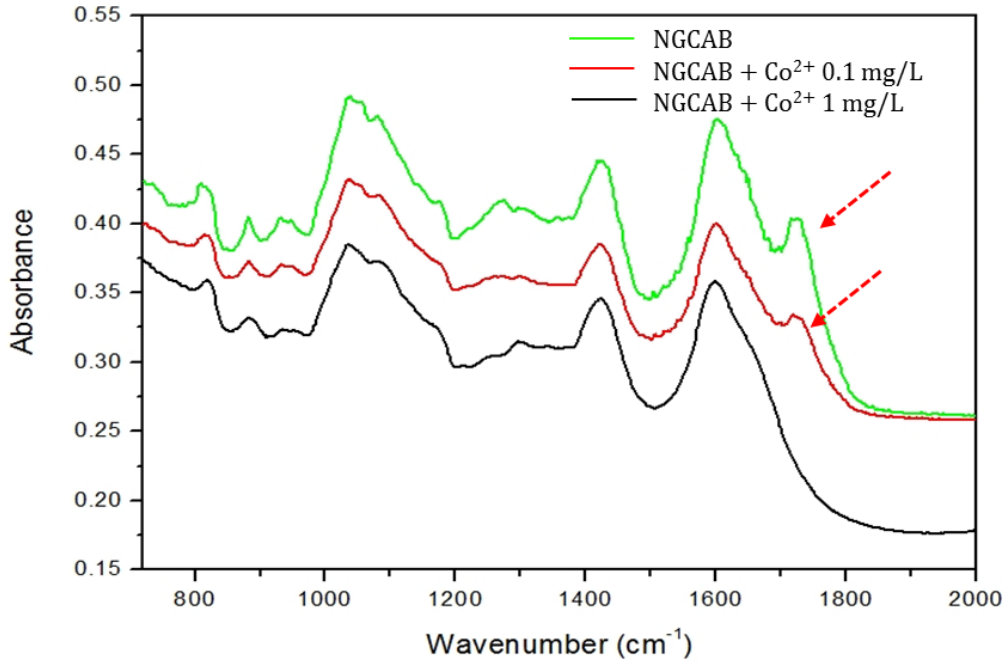

Figure 4. FT-IR spectra of nano-scale carbon alginate bead

4.3 Adsorption studies

The sorption rate is known to be controlled by several factors including the following;(I) diffusion of the solute from the solution to the film surrounding the particle, (II) diffusion from the film to the particle surface (external diffusion), (III) diffusion from the surface to the internal sites (surface diffusion or pore diffusion) and (IV) uptake which can involve several mechanisms such as physic-chemical sorption, ion exchange, precipitation or complexation.

4.3.1 Effect of pH

Important parameter of pH was controlled in this study to confirm adsorption of metal ions onto the liquid/solid interface. As a result, surface properties of the adsorbent were affected by pH which influences the metal speciation in solution. Co^{2+} appeared as Co^{2+} below pH 7.8, while $Co(OH)^{+}$ and $Co(OH)_2$ were the dominant form at pH values between 7.8 and 10, and Co^{2+} existed as $Co(OH)_3^{-}$ above pH 10 [63] whereupon Co^{2+} has the speciation profile of Co^{2+} at different pH values in aqueous phase. In the Fig. 5, between pH 5 and 9 NGCAB appeared higher adsorption capacity than AB that was attributed to increased pore area of the alginate beads impregnated with NGC also at pH 2 to 3 AB and NGCAB had low Co^{2+} adsorption affinity due to the competition between H^{+} and Co^{2+} for opposite sites on the surface of adsorbent and/or the charge reversal of the adsorbent surface under those acidic conditions. The optimal adsorption was at pH7 during increasing solution pH from 3 to 7. That's why deprotonation of the adsorbent surface at same time increasing Co^{2+} adsorption with pH. The deprotonation starting at pH 3 resulted in increased amount of negatively-charged sites upon the absorbent surface. Also in the pH range 7 to 9 was steady of Co^{2+} adsorption that indicating a possible Co^{2+} precipitation along with adsorption [64]. The optimum pH condition for Co^{2+} adsorption was also confirmed through Hard-

Soft-Acid-Base theory [65]. In general oxygen containing functionalities (soft bases) such as carbonyl, carboxyl, and hydroxyl groups dominates over the surface of carbonaceous adsorbents. These functionalities will co-ordinate with soft acids (such as Co^{2+} and $Co(OH)^{+}$) in the aqueous phase [66]. At below pH 7, these soft acid functionalities are the dominating species in aqueous medium confirming active involvement of these species adsorption process.

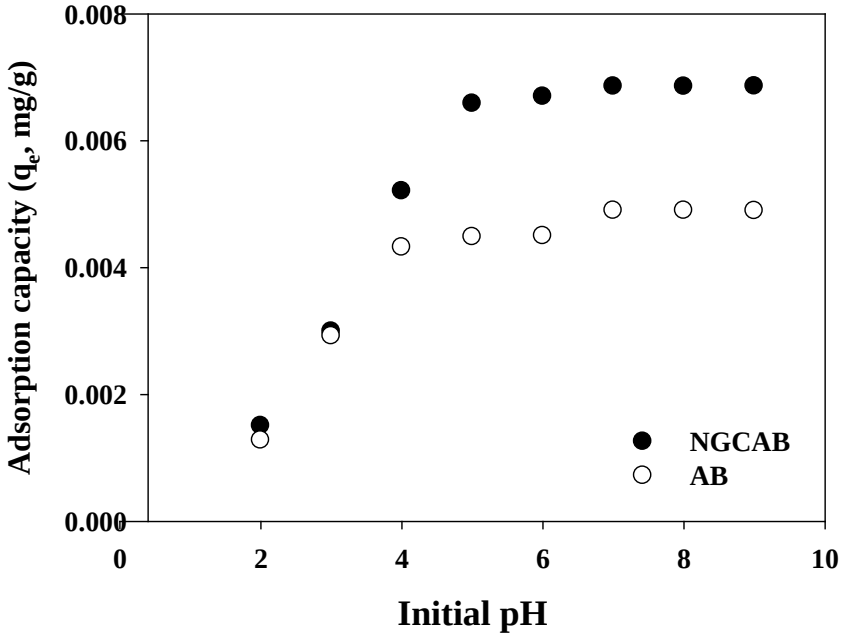

Figure 5. pH dependence of Co^{2+} adsorption on AB and NGCAB

4.3.2 Effect of contact time

To determinate the function of contact time of NGCAB and AB as initial Co^{2+} concentrations ranging from 0.1 to 200 mg/L and different thermal conditions (288 to 318 K). In the Fig. 6, the equilibrium time was 10 to 15days irrespective of the type of adsorbents. The initial Co^{2+} adsorption on NGCAB was particularly faster than later adsorption because of great deal of possible adsorption sites at equilibrium. Also, chemisorption process is more dominant at initial stage of fast Co^{2+} adsorption on NGCAB. The adsorption capacity of NGCAB increased from 0.0072 to 5.756 mg/g with increasing the initial Co^{2+} concentration from 0.1 to 200 mg/L.

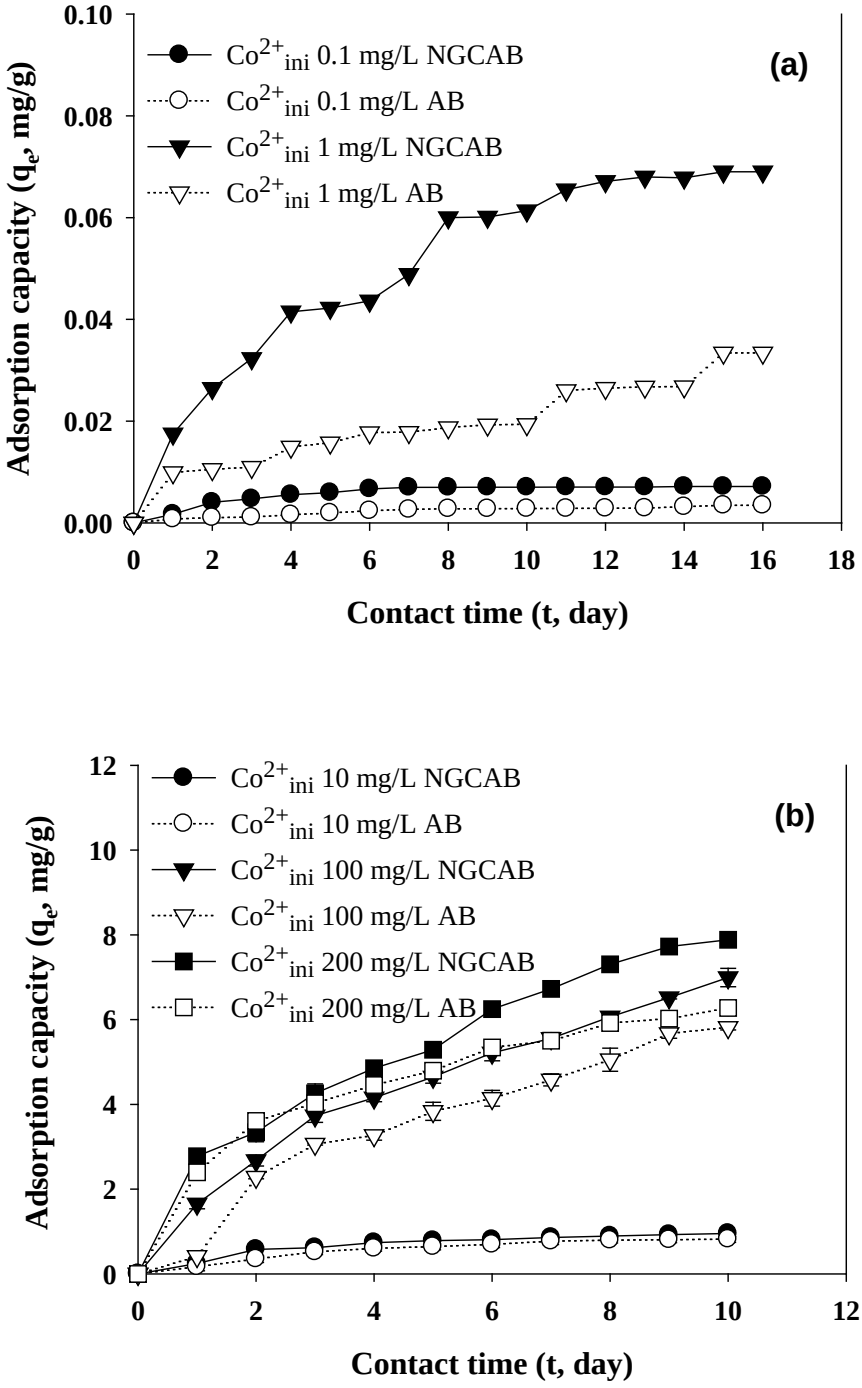

Figure 6. Effects of initial Co^{2+} concentrations on the adsorption capacity as a function of time. The initial concentrations of Co^{2+} ranged from 0.1 to 1 mg/L (a) and from 10 to 200 mg/L (b)

At various initial Co^{2+} concentrations were estimated using using pseudo-first-order and pseudo-second-order kinetics models. Pseudo-first-order kinetics model also known as Lagergren kinetics model in linearized form can be expressed as [67]:

$$\log(q_e - q_t) = \log q_e - \frac{k_1}{2.303} \times t \quad (2)$$

where, K_1 (1/min) is pseudo-first-order rate constant, q_e and q_t (mg/g) are the adsorption capacities at equilibrium and time *t*, respectively.

Pseudo-second-order kinetic model was used in linearized form by Ho and Mc Kay expressed as [68]:

$$\frac{t}{q_t} = \frac{1}{h} + \frac{t}{q_e} \quad (3)$$

$$h = k_2 q_e^2 \quad (4)$$

where, K_2 (g/mg-min) is the pseudo-second-order rate constant, and *h* (mg/g min) is initial sorption rate. The regression coefficient (R^2) values (Table 2 (a and b)) for pseudo-second-order model were relatively higher compared to those for pseudo-first-order model. The higher R^2 values confirmed the applicability of pseudo-second- order model at various Co^{2+} concentrations ranging from 0.1 to 200 mg/L. This further confirmed that Co^{2+} adsorption onto AB and NGCAB was chemisorption process. The pseudo-second-order adsorption rate constant (K_2) gradually decreased as the initial Co^{2+} concentration was increased. The decline in K_2 was due in part to promotion of the competition for adsorption sites at high Co^{2+} concentrations.

Table 2. Pseudo-first-order (a) and Pseudo-second-order (b) kinetics parameters for Co^{2+} adsorption onto AB and NGCAB at different concentrations.

Co^{2+} (mg/L)	q_e(exp)(mg/g)		q_e(theo)(mg/g)		K_1(1/min)		R^2	
	AB	NGCAB	AB	NGCAB	AB	NGCAB	AB	NGCAB
0.1	0.0035	0.0071	0.0031	0.0064	0.1567	0.3823	0.927	0.898
1	0.0334	0.0603	0.0299	0.1057	0.1066	0.3104	0.899	0.934
10	0.6078	0.7518	1.335	0.9759	0.4834	0.3609	0.949	0.958
100	3.8507	5.7559	5.947	7.9341	0.3272	0.2736	0.957	0.948
200	4.472	5.7822	8.3215	11.4657	0.3365	0.3823	0.8	0.862

Co^{2+} (mg/L)	q_e(exp)(mg/g)		q_e(theo)(mg/g)		K_2		R^2	
	AB	NGCAB	AB	NGCAB	AB	NGCAB	AB	NGCAB
0.1	0.0035	0.0071	0.0049	0.008	27.711	78.517	0.934	0.995
1	0.0334	0.0603	0.2417	0.0942	0.169	1.966	0.97	0.979
10	0.6078	0.7518	0.9858	1.0276	0.166	0.25	0.969	0.992
100	3.8507	5.7559	8.6805	13.055	0.009	0.005	0.96	0.959
200	4.472	5.7822	15.174	34.13	0.003	0.001	0.813	0.879

4.3.3 Thermodynamics studies

In three different temperature conditions, the contact time studies were performed at 0.1 mg/L of Co^{2+} concentration. As a result of reaction temperature (Fig. 7 a and b), AB and NGCAB was increased from 0.0027 to 0.0066 mg/g with temperature from 288 to 318 K. This result was negligible under the examined temperatures but the result revealed that adsorption process is endothermic in nature.

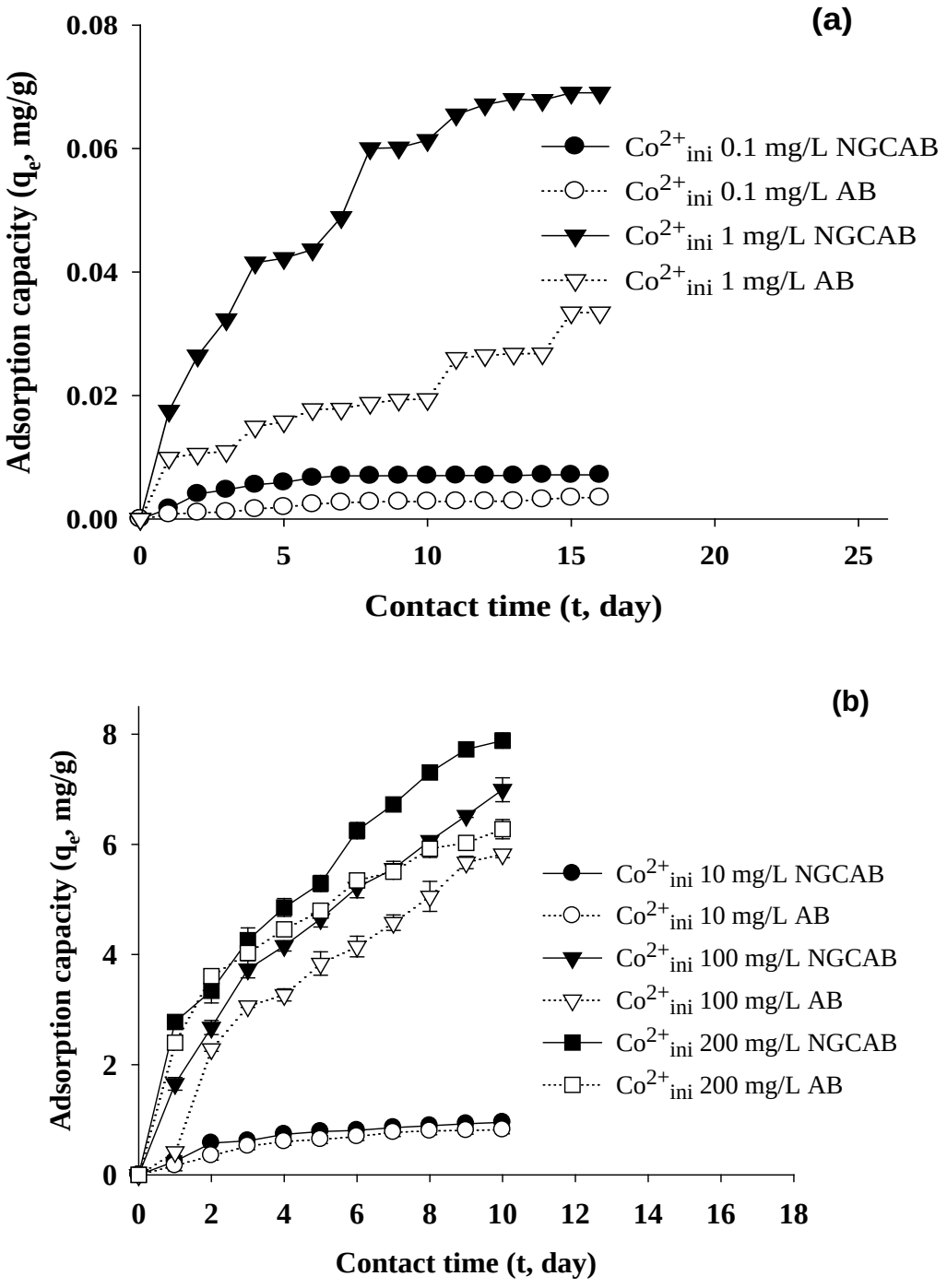

Figure 7. Effects of thermal conditions as a function of time on adsorption capacity of AB (a) and NGCAB (b) for Co^{2+}

Various thermodynamics parameters such as Gibb's free energy (*ΔG°*), standard enthalpy change (*ΔH°*), and standard entropy change (*ΔS°*) were evaluated.

Gibb's free energy (*ΔG°*) was calculated using Eq. 5.

$$\Delta G^0 = -RT \ln K_c \tag{5}$$

$$\ln K_c = \frac{C_{Ae}}{C_e} \tag{6}$$

where, C_{Ae} and C_e (mg/L) are the Co^{2+} concentrations onto adsorbent and in the solution, respectively.

Von't Hoff equation was used to evaluate the *ΔH°* and *ΔS°* values. The equation is expressed as:

$$\ln K_c = \frac{\Delta S^0}{R} - \frac{\Delta H^0}{RT} \tag{7}$$

Results showed that adsorption process on both AB and NGCAB was endothermic in nature as revealed by positive *ΔH°* values. The Co^{2+} adsorption onto the solid phase needs destruction of hydration sheath around the ion, and the endothermic nature of the process showed that the energy is required of dehydration process which is favorable at high temperature [69]. The implicit assumption is that after adsorption the environment of Co^{2+} ions is less aqueous phase. The endothermicity of the desolvation process becomes higher than the enthalpy of adsorption because the removal of water from Co^{2+} ions is substantially an endothermic process [70]. The ΔG° values for Co^{2+} adsorption onto NGCAB were negative in the range 288 to 318 K, while onto AB the ΔG° showed negative value only at 318 K. The decline in ΔG° values was due to

hydrolysis of Co^{2+} ions at high temperature. The positive ΔS° values imply that some structural changes in adsorbate and adsorbent were occurred during the adsorption process, which was possibly attributed to the increase in the randomness at the solid/solution interface.

Dubinin and Radushkevich (D-R) model [71] was used to estimate activation energy (Ea, kJ/mol) of the adsorption process. The D-R model in linearized form is given as:

$$\ln q_e = \mathrm{B}\varepsilon^2 + \ln q_m \tag{8}$$

where, Ɛ is the Polanyi potential, q_e is the adsorption capacity (mmol/g), q_m is the theoretical adsorption capacity (mmol/g), and the Polanyi potential values was determined by using Eq. (9):

$$\varepsilon = RT \ln\left(1 + \frac{1}{C_e}\right) \tag{9}$$

where, C_e is equilibrium concentration of Co^{2+} (mmol/L)

The E_a values were obtained by E_q (10):

$$E_a = \frac{1}{\sqrt{-2\mathrm{B}}} \tag{10}$$

The Ea values for Co^{2+} adsorption onto AB and NGCAB were 8.451 and 22.36 kJ/mol, indicating that the adsorption of Co^{2+} onto AB and NGCAB was chemical adsorption.

Table 3. Thermodynamics parameters for Co^{2+} adsorption onto AB and NGCAB

Adsorbent	Temperature (K)	ln K_c	ΔH°(kJ/mol)	ΔS°(kJ/mol-K)	ΔG°(kJ/mol)
AB	288	-0.964	7.536	0.033	2.309
	298	-0.299			0.741
	318	0.653			-1.728
NGCAB	288	0.826	40.418	0.132	-1.978
	298	0.928			-2.299
	318	1.124			-2.972

4.3.4 Effect of concentration and isotherm studies

The Co^{2+} adsorption onto AB and NGCAB was studied by varying initial Co^{2+} concentration (0.01-200 mg/L). The adsorption capacity of NGCAB varied from 0.00067 to 2.414 mg/g for the assigned concentration range, while the adsorption capacity of AB accounted for 0.00052 to 1.724 mg/g (Fig. 8). Increasing Co^{2+} adsorption with stepped the initial concentration suggested that an increase in Co^{2+} concentration improved a driving force to overcome mass transfer resistant barrier between solid/aqueous phases.

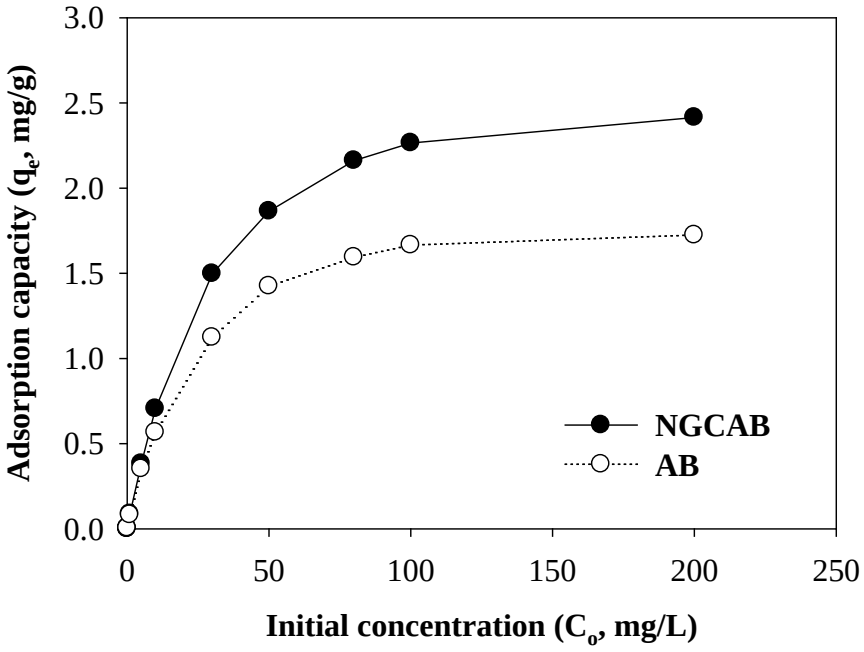

Figure 8. Adsorption capacity of AB and NGCAB as a function of initial Co^{2+} concentration

The two parameters Langmuir, Freundlich, and Temkin isotherm models were applied to experimental data. Langmuir isotherm assumes monomolecular layer formation during adsorption process without interaction between the adsorbed molecules. Langmuir isotherm in linearized form is represented as [72].

$$\frac{C_e}{q_e} = \frac{1}{bq_m} + \frac{1}{q_m} \times C_e \tag{11}$$

where, C_e is concentration of adsorbate at equilibrium (mg/L), q_e is adsorption capacity at equilibrium (mg/g), q_m is Langmuir constant for maximum solid phase loading on adsorbent (mg/g) and b is Langmuir constant related to heat of adsorption (L/mg).

The essential feature of Langmuir isotherm can be expressed in terms of separation factor (R_L).

$$R_L = \frac{1}{1 + bC_o} \tag{12}$$

Separation factor (R_L), a dimensionless constant. If, R_L >1.0 - unfavourable adsorption, 0< R_L <1.0 - favourable adsorption, R_L = 1.0 - linear adsorption and R_L = 0 - irreversible adsorption.

Freundlich isotherm assumes that the adsorption occurred on the heterogeneous surface sites. Freundlich isotherm in linearized form is expressed as [73].

$$\log q_e = \log k_F + \frac{1}{n} \log C_e \tag{13}$$

where, K^f ((mg/g)(L/mg)$^{(1/n)}$) and n are the Freundlich constants which are

related to bonding energy.

Temkin isotherm assumes linear decrease in adsorption energy along with the saturation of adsorption sites present over the surface of adsorbent rather than exponential decrease as implied by Freundlich isotherm. Temkin isotherm contains a factor that explicitly takes into account the adsorbing species-adsorbate interactions and the isotherm is given by linearized expression as.

$$q_e = B_T \ln K_T + B_T \ln C_e \tag{14}$$

where, B_T = RT/b, R is the universal gas constant (8.314 J/mol-K), T is the absolute temperature (K), b is Temkin constant related to adsorption energy (kJ/mol), K_T is the binding constant at equilibrium corresponding to the maximum binding energy (L/g).

Results showed that Langmuir model was best fitted to experimental data as supported by higher R^2 values (Table. 4) regardless of the type of adsorbent. This was further confirmed with nearer experimental and theoretical values of Langmuir constant (q_m). The values of R_L were in the range of favorable adsorption onto AB and ABGNC. The Freundlich constant (n) values ranged between 1.0 and 10, further confirming the favorable adsorption process.

Table 4. Isotherm data for Co^{2+} adsorption onto AB and NGCAB

Isotherm	Adsorbent	
	AB	NGCAB
Langmuir		
q_m (theo) (mg/g)	1.852	2.524
q_m (exp) (mg/g)	1.724	2.414
b (L/g)	0.0849	0.1133
R_L	0.056 – 0.999	0.042 – 0.999
R^2	0.9905	0.9978
Freundlich		
K^f (mg/g)(L/mg)$^{1/n}$	0.0863	0.1415
n	1.305	1.361
R^2	0.9103	0.9247
Temkin		
B_1	0.1934	0.2542
K_T (L/mg)	24.337	33.717
R^2	0.8867	0.8797

5. Conclusion

As adsorbent, nano-size graphite carbon (NGC) was successfully impregnated in alginate bead (AB). In aqueous solution Co^{2+} ion could remove using NGCAB and AB. The Co^{2+} adsorption was most effective at pH 7 among the examined pH values ranging from 2 to 9, which reached equilibrium time almost 10 days. The chemisorption process for Co^{2+} adsorption was confirmed from the initially fast adsorption rate, implicated with an electrostatic interaction between $–COO^-$ and Co^{2+} ions. The Co^{2+} adsorption capacity of both NGCAB and AB increased from 0.0072 to 5.756 mg/g and from 0.0034 to 4.472 mg/g as the initial Co^{2+} concentration was increased from 0.1 to 200 mg/L. Endothermic nature of the adsorption was confirmed from the progressive increase in Co^{2+} adsorption, and the pseudo-second-order kinetic model was also well-fitted to the experimental data. Langmuir model gave a better fit to the experimental data than other isotherm equations and the positive values of entropy disclose that some structural changes occurred in adsorbate and adsorbent during adsorption process.

6. Reference

[1] H. Ghassabzadeh, M. T. Mostaedi, A. Mohaddespour, M. G. Maragheh, S. J. Ahmadi, P. Zaheri, Characterizations of Co (II) and Pb (II) removal process from aqueous solutions using expanded perlite, Desalination. 261 (2010), 73–79

[2] E. Repo, J. K. Warchol, T. A. Kurniawana, M. E. T. Sillanpää, Adsorption of Co(II) and Ni(II) by EDTA- and/or DTPA-modified chitosan: Kinetic and equilibrium modeling, Chem. Eng. J. 161 (2010), 73–82

[3] A. Naeem, M.T. Saddique, S. Mustafa, S. Tasleem, K.H. Shah, M. Waseem, Removal of Co^{2+} ions from aqueous solution by cation exchange sorption onto NiO, J. Hazard. Mater. 172 (2009), 124–128.

[4] A. Olgun, N. Atar, Removal of copper and cobalt from aqueous solution onto waste containing boron impurity, Chem. Eng. J. 167 (2011), 140–147

[5] M. He, Y. Zhu, Y. Yang, B. Han, Y. Zhang, Adsorption of cobalt(II) ions from aqueous solutions by palygorskite, Appl. Clay. Sci. 54 (2011), 292–296

[6] M. Monier, D.M. Ayad, Y. Wei, A.A. Sarhan, Adsorption of Cu(II), Co(II), and Ni(II) ions by modified magnetic chitosan chelating resin, J. Hazard. Mater. 177 (2010), 962–970

[7] Eveliina Repo, Roman Petrus, Mika Sillanpää, Jolanta K. Warchoł, Equilibrium studies on the adsorption of Co(II) and Ni(II) by modified silica gels: One-component and binary systems, Chem. Eng. J. 172 (2011), 376– 385

[8] A. F. Ngomsika, A. Bee, J. M. Siaugue, V. Cabuil, G. Cote, Nickel adsorption by magnetic alginate microcapsules containing an extractant, Water Res. 40 (2006), 1848–1856

[9] D. Zhou, L. Zhang, J. Zhou, S. Guo, Cellulose/chitin beads for adsorption of

heavymetals in aqueous solution, Water Res. 38 (2004), 2643–2650

[10] K. Swayampakula, V. M. Boddu, S. K. Nadavala, K. Abburi, Competitive adsorption of Cu (II), Co (II) and Ni (II) from their binary and tertiary aqueous solutions using chitosan-coated perlite beads as biosorbent, J. Hazard. Mater. 170 (2009), 680–689

[11] C. Gok, S. Aytas, Biosorption of uranium (VI) from aqueous solution using calcium alginate beads, J. Hazard. Mater. 168 (2009), 369-375

[12] T. Gotoh, K. Matsushima, K. I. Kikuchi, Adsorption of Cu and Mn on covalently cross-linked alginate gel beads, Chemosphere. 55 (2004), 57–64

[13] G. Jegadeesan, S. R. Al-Abed, V. Sundaram, H. Choi, K. G. Scheckel, D. D. Dionysiou, Arsenic sorption on TiO_2 nanoparticles: Size and crystallinity effects, Water Res. 44 (2010), 965–973

[14] R. Selvakumar, N. Arul Jothi, V. Jayavignesh, K. Karthikaiselvi, Geny Immanual Antony, P.R. Sharmila, S. Kavitha, K. Swaminathan, As(V) removal using carbonized yeast cells containing silver nanoparticles, Water Res. 45 (2011), 583-592

[15] G. A. Waychunas, C. S. Kim, J. F. Banfield, Nanoparticulate iron oxide minerals in soils and sediments: unique properties and contaminant scavenging mechanisms, J. Nanopart. Res. 7 (2005), 409–433

[16] M. Bahgat, A. A. Farghali, W. M. A. El Rouby, M. H. Khedr, Synthesis and modification of multi-walled carbon nano-tubes (MWCNTs) for water treatment applications, J. Anal. Appl. Ryrol. 92 (2011), 307–313

[17] A. Karagunduz, Y. Kaya, B. Keskinler, S. Oncel, Influence of surfactant entrapment to dried alginate beads on sorption and removal of Cu^{2+} ions , J. Hazard. Mater. B131 (2006), 79–83

[18] S. K. Nadavala, K. Swayampakula, V. M. Boddu, K. Abburi, Biosorption of phenol and o-chlorophenol from aqueous solutions on to chitosan–calcium alginate blended beads, J. Hazard. Mater. 162 (2009), 482–489

[19] Y. B. Lin, B. Fugetsu, N. Terui, S. Tanaka, Removal of organic compounds by alginate gel beads with entrapped activated carbon, J. Hazard. Mater. B120 (2005), 237–241

[20] V. Rocher, A. Bee, J. M. Siaugue, V. Cabuil, Dye removal from aqueous solution by magnetic alginate beads crosslinked with epichlorohydrin, J. Hazard. Mater. 178 (2010), 434–439

[21] D. M. Manohar, B. F. Noeline, T. S. Anirudhan, Adsorption performance of Al-pillared bentonite clay for the removal of cobalt(II) from aqueous phase, Appl. Clay. Sci. 31 (2006), 194–206

[22] I. Smiciklas, S. Dimovic, I. Plecas, M. Mitric, Removal of Co^{2+} from aqueous solutions by hydroxyapatite, Water Res. 40 (2006), 2267–2274

[23] A. Khan, S., Sorption of the long-lived radionuclides cesium-134, strontium-85 and cobalt-60 on bentonite, J. Radioanal. Nucl. Che. 258 (2003), 3–6.

[24] S. E. Bailey, T. J. Olin, R. M. Brick and D. D. Adrian, Review of potentially low-cost sorbents for heavy metals, Water Res. 33 (1999), 2469-2479

[25] A. Bhatnagar, A.K. Minocha, M. Sillanpää, Adsorptive removal of cobalt from aqueous solution by utilizing lemon peel as biosorbent, Biochem. Eng. J. 48 (2010), 181–186

[26] J. L. Huisman, G. Schouten, C. Schultz, Biologically produced sulphide for purification of process streams, effluent treatment and recovery of metals in the metal and mining industry, Hydrometallurgy. 83 (2006), 106–113

[27] K. A. Baltpurvins, R. C. Burns, G. A. Lawrance and A. D. Stuart, Effect of

electrolyte composition on zinc hydroxide precipitation by lime, Water Res. 31 (1997), 973–980

[28] A. O¨ zverdi, M. Erdem, Cu^{2+}, Cd^{2+} and Pb^{2+} adsorption from aqueous solutions by pyrite and synthetic iron sulphide, J. Hazard. Mater. B137 (2006) 626–632

[29] S. Y. Kang, J. U. Lee, S. H. Moon, K. W. Kim, Competitive adsorption characteristics of Co^{2+}, Ni^{2+}, and Cr^{3+} by IRN-77 cation exchange resin in synthesized wastewater, Chemosphere. 56 (2004), 141–147

[30] B. Alyüz, S. Veli, Kinetics and equilibrium studies for the removal of nickel and zinc from aqueous solutions by ion exchange resins, J. Hazard. Mater. 167 (2009), 482–488

[31] H. Bessbousse, T. Rhlalou, J. F. Verch`ere, L. Lebrun, Removal of heavy metal ions from aqueous solutions by filtration with a novel complexing membrane containing poly (ethyleneimine) in a poly (vinyl alcohol) matrix, J. Membrane. Sci. 307 (2008), 249–259

[32] M.A. Barakat, E. Schmidt, Polymer-enhanced ultrafiltration process for heavy metals removal from industrial wastewater, Desalination. 256 (2010), 90–93

[33] J. L. Aguirre, V. García, E. Pongracz, R. L. Keiski, The removal of zinc from synthetic wastewaters by micellar-enhanced ultrafiltration: statistical design of experiments, Desalination. 240 (2009), 262-269

[34] M.A. Barakat, E. Schmidt, Polymer-enhanced ultrafiltration process for heavy metals removal from industrial wastewater, Desalination. 256 (2010) 90–93

[35] L. Yurlova, A. Kryvoruchko, B. Kornilovich, Removal of Ni(I1) ions from wastewater by micellar-enhanced ultrafiltration, Desalination. 144 (2002), 255-

260

[36] C. O. Do anay, H. Ö. Özbelge, L. Yilmaz, N. Biçak, Removal and recovery of metal anions via functional polymer based PEUF, Desalination. 200 (2006), 286–287

[37] A. P. Kryvoruchko, I. D. Atamanenko, L. Yu. Yurlova, Concentration/purification of Co(II) ions by reverse osmosis and ultrafiltration combined with sorption on clay mineral montmorillonite and cation-exchange resin KU-2-8n, J. Membrane. Sci. 228 (2004), 77–81

[38] S. Bouranene, P. Fievet, A. Szymczyk, M. E. H. Samar, A. Vidonne, Influence of operating conditions on the rejection of cobalt and lead ions in aqueous solutions by a nanofiltration polyamide membrane, J. Membrane. Sci. 325 (2008), 150–157

[39] E. Assaad, A. Azzouz, D. Nistor, A.V. Ursu, T. Sajin, D.N. Miron, F. Monette, P. Niquette, R. Hausler, Metal removal through synergic coagulation–flocculation using an optimized chitosan–montmorillonite system, Appl. Clay. Sci. 37 (2007), 258–274

[40] Q. Chang, G. Wang, Study on the macromolecular coagulant PEX which traps heavy metals, Chem. Eng. Sci. 62 (2007), 4636–4643

[41] Q. Chang, M. Zhang, J. Wang, Removal of Cu^{2+} and turbidity from wastewater by mercaptoacetyl chitosan, J. Hazard. Mater. 169 (2009), 621–625

[42] Donald L. Sparks., 1995. Environmental soil chemistry, Academic press, San Diego

[43] Findon, A., Mckay, O., Blair, H. S. Transport studies for the sorption of copper ions by chitosan. J. Environ. Sci. Heal. A. 28 (1993), 173-185

[44] X. Li, Y. Li, Z. Ye, Preparation of macroporous bead adsorbents based on

poly(vinyl alcohol)/chitosan and their adsorption properties for heavy metals from aqueous solution, Chem. Eng. J. 178 (2011), 60– 68

[45] Z. Y. Lin, Y. X. Zhang, Y. L. Chen, H. Qian, Extraction and recycling utilization of metal ions (Cu^{2+}, Co^{2+} and Ni^{2+}) with magnetic polymer beads, Chem. Eng. J. 200–202 (2012), 104–112

[46] N, Lazaro, A, L, Sevilla, S, Morales, A, M. Marques, Heavy metal biosorption by gellan gum gel beads, Water Res. 37 (2003), 2118–2126

[47] J. Dai, H. Yang, H. Yan, Y. Shangguan, Q. Zheng, R. Cheng, Phosphate adsorption from aqueous solutions by disused adsorbents: Chitosan hydrogel beads after the removal of copper (II), Chem. Eng. J. 166 (2011), 970–977

[48] A. Kara, L. Uzun, Necati Besirli, A. Denizli, Poly (ethylene glycol dimethacrylate-n-vinyl imidazole) beads for heavy metal removal, J. Hazard. Mater. 106B (2004), 93–99

[49] L. Gottlieb, Preparation, morphology and function of biomass filled porous epoxy beads as chelation-ion-exchange for lead ion sorption, React. Funct. Polym. 63 (2005), 107–117

[50] W. S. Wan Ngah, C. S. Endud, R. Mayanar, Removal of copper(II) ions from aqueous solution onto chitosan and cross-linked chitosan beads, React. Funct. Polym. 50 (2002), 181–190

[51] A. Haug, B. Larsen and O. Smidsrod, A study of the constitution of alginic acid by partial acid hydrolysis, Acta chemical scandinavica 20 (1966) 183–190

[52] Arne Haug, Bjorn Larsen and Olave Smidsrod, Correlation between chemical structure and physical properties of alginates, Acta. Chem. Scand. 21 (1967), 768–778

[53] A. Haug, B. Larsen and O. Smidsrod, Uronic acid sequence in alginate from

different sources, Carbohyd. Res. 32 (1974), 217–225

[54] D. A. Rees, Polysaccharide shape and their interactions some recent advances, Pure. Appl. Chem. 53 (1981), 1–14

[55] A. Rahmani, H. Zavvar Mousavi, M. Fazli, Effect of nanostructure alumina on adsorption of heavy metals, Desalination 253 (2010), 94–100

[56] J. P. Ruparelia, S. P. Duttagupta, A. K. Chatterjee, S. Mukherji, Potential of carbon nanomaterials for removal of heavy metals from water, Desalination 232 (2008) 145–156

[57] A. F. Ngomsik, A. Bee, J. M. Siaugue, D. Talbot, V. Cabuil, G. Cote, Co(II) removal by magnetic alginate beads containing Cyanex 272®, J. Hazard. Mater. 166 (2009), 1043–1049

[58] H. G. Park, T. W. Kim, M. Y. Chae, I. K. Yoo, Activated carbon-containing alginate adsorbent for the simultaneous removal of heavy metals and toxic organics, Process. Biochem. 42 (2007), 1371–1377

[59] T. Gotoh, K. Matsushima, K. I. Kikuchi, Preparation of alginate–chitosan hybrid gel beads and adsorption of divalent metal ions, Chemosphere. 55 (2004), 135–140

[60] C. Escudero, N. Fiol, I. Villaescusa, J. C. Bollinger, Arsenic removal by a waste metal (hydr)oxide entrapped into calcium alginate beads, J. Hazard. Mater. 164 (2009), 533–541

[61] T. S. Pathak, J. H. Yun, S. J. Lee, D. J. Baek, K. J. Paeng, Effect of cross-linker and cross-linker concentration on porosity, surface morphology and thermal behavior of metal alginates prepared from algae (Undaria pinnatifida), Carbohyd. Polym. 78 (2009), 717–724

[62] Pathak, T. S., Yun, J. H., Lee, S. J., Baek, D. J., and Paeng, K.-J. Effect of

cross-linker and cross-linker concentration on porosity, surface morphology and thermal behavior of metal alginates prepared from algae (Undaria pinnatifida), Carbohyd. Polym. 78 (2009), 717–724.

[63] A. N. Bezbaruah, S. Krajangpan, B. J. Chisholm, E. Khan, J. J. Elorza Bermudez, Entrapment of iron nanoparticles in calcium alginate beads for groundwater remediation applications, J. Hazard. Mater. 166 (2009), 1339–1343

[64] K. Pyrzyn´ska, M. Bystrzejewski, Comparative study of heavy metal ions sorption onto activated carbon, carbon nanotubes, and carbon-encapsulated magnetic nanoparticles, Colloid. Surface. A. 362 (2010), 102–109

[65] W. Liu, J. Zhang, C. Cheng, G. Tian, C. Zhang, Ultrasonic-assisted sodium hypochlorite oxidation of activated carbons for enhanced removal of Co(II) from aqueous solutions, Chem. Eng. J. 175 (2011), 24– 32

[66] R. G. Pearson, Absolute Electronegativity and Hardness: Application to Inorganic Chemistry, Inorg. Chem. 27 (1988), 734-740

[67] R. L. Tseng, F. C. Wu, R. S. Juang, Characteristics and applications of the Lagergren's first-order equation for adsorption kinetics, J. Taiwan. Inst. Chem. E 41 (2010), 661–669

[68] Y. S. HO and G. MCKAY, The kinetics of sorption of divalent metal ions onto sphagnum moss peat, Water Res. 34(2000), 735–742

[69] Q. Wang, J. Li, C. Chen, X. Ren, J. Hu, X. Wang, Removal of cobalt from aqueous solution by magnetic multi walled carbon nanotube/iron oxide composites, Chem. Eng. J. 174 (2011), 126–133

[70] Z. Guo, Y. Li, S. Zhang, H. Niu, Z. Chen, J. Xu, Enhanced sorption of radiocobalt from water by Bi(III) modified montmorillonite: A novel adsorbent, J. Hazard. Mater. 192 (2011), 168–175

[71] M. M. Dubinin, L. V. Radushkevich, The equation of the characteristic curve of the activated charcoal, Proc. Acad. Sci. USSR Phys. Chem. Sect. 55 (1947), 331–337

[72] I. Langmuir, The adsorption of gases on plane surface of glass, mica and platinum. J. Am. Chem. Soc. 40 (1916), 1361–1403

[73] M. I. Tempkin, V. Pyzhev, Kinetics of ammonia synthesis on promoted iroi catalyst, Acta Phys. Chim. USSR 12 (1940), 327–356

국 문 요 약

NGCAB를 이용한 수용액상의 Co^{2+} 이온 흡착제거연구

흡착제로써 나노크기의 그래파이트 카본을 성공적으로 알지네이트비드에 첨착하여 사용하였고 수용액상의 코발트 이온은 NGCAB와 비교군으로 사용된 AB에 의해 잘 제거되었다. 코발트 흡착은 pH 7에서 흡착효율이 가장 좋았으며 약 10일의 흡착평형시간을 보였다. $–COO^-$와 Co^{2+} 간의 정전기적 상호작용에 의해 초기 코발트 흡착율이 증가하였다. 코발트 흡착량은 초기 농도 0.1 ~ 200 mg/L로 증가함에 따라 0.0072에서 5.756 mg/g, 0.0034에서 4.472 mg/g으로 각각 증가하였으며 흡착등온모델을 이용하였을 시에 Langmuir 모델에 가장 적합하게 나타났다. 또한 시간에 따른 흡착을 관찰해 본 결과 Pseudo-second-order 모델에서 가장 잘 표현할 수 있었으며 약 10일이상의 느린 흡착은 알지네이트 표면흡착과 나노카본에 의한 흡착에 의해 느린 것으로 사료된다.

핵심되는 말 : (흡착, 코발트, 알지네이트, 나노)